Research Square

Preprints are preliminary reports that have not undergone peer review.
They should not be considered conclusive, used to inform clinical practice,
or referenced by the media as validated information.

Proteome-wide evolutionary rate covariation reveals the mitonuclear coevolutionary landscape in Squamata

Oscar Wallnoefer

oscar.wallnoefer2@unibo.it

University of Bologna

Mirko Martini

University of Bologna

Giorgia Galletti

University of Bologna

Nicolò Gabriele

University of Bologna

Marco Passamonti

University of Bologna

Federico Plazzi

University of Bologna

Research Article

Keywords: mitonuclear coevolution, evolutionary rates covariation, ERC, phylogenetic discordance, Squamata, mitochondria

Posted Date: March 25th, 2026

DOI: https://doi.org/10.21203/rs.3.rs-9148480/v1

License: This work is licensed under a Creative Commons Attribution 4.0 International License.
Read Full License

Additional Declarations: No competing interests reported.

Abstract

The reciprocal evolutionary adjustment between mitochondrial and nuclear genomes is well characterized at the oxidative phosphorylation (OXPHOS) interface, yet the extent to which mitonuclear coevolution extends beyond mitochondrial pathways remains largely unknown. Evolutionary Rate Covariation (ERC) can detect long-term coevolutionary relationships by identifying protein pairs whose evolutionary rates covary across a phylogeny, but its proteome-wide applications have so far been limited to a few taxa. Here, we scaled ERC to nearly three million protein pairs across 34 squamate proteomes, reconstructing a proteome-wide coevolutionary network.

Mitochondrial OXPHOS genes emerge as network hubs, and their coevolutionary neighborhoods extend well beyond the oxidative phosphorylation pathway into calcium signaling, peroxisomes, and pigmentation-related genes, a signal robust even at high correlation stringency. In squamates, coloration plays roles in courtship signaling and UV protection. The coevolutionary association between mitochondrial OXPHOS genes and nuclear genes involved in pigmentation may be consistent with the mitonuclear ecology hypothesis, which posits that ornamental coloration advertises cellular respiratory efficiency.

We further exploited the deep mitonuclear phylogenetic discordance of Squamata to test whether coevolution also leaves topological signatures in gene trees. Nuclear genes supporting the mitochondrial topology were short and phylogenetically poorly informative, suggesting stochastic rather than coevolutionary discordance.

Together, these results demonstrate that ERC captures functional coevolution that topology-based approaches miss, and reveal that the evolutionary reach of mitochondria extends beyond OXPHOS.

BACKGROUND

Mitochondria and the nucleus have been coevolving for approximately two billion years following the endosymbiotic event between a heterotrophic archaeon and an aerobic alpha-proteobacterium (Williams and Embley 2014; Hill 2019). Mitochondria are best-known as the site of oxidative phosphorylation (OXPHOS), the primary ATP-producing pathway in eukaryotic cells. Since four of the five OXPHOS complexes are assembled from both nuclear- and mitochondrial-encoded subunits (nucOXPHOS and mtOXPHOS; the second complex has only nuclear origin), and since this pathway is essential across eukaryotes, changes in one genome can impose compensatory mutations in the other one, resulting in continuous mitonuclear coevolution (Gershoni et al., 2010; Sloan et al., 2018; Hill 2020). This ancient cooperation has resulted in the OXPHOS pathway emerging as an ideal model for investigating mitonuclear coevolution (Yan et al., 2019; Piccinini et al., 2021; Weaver et al., 2022; Gonçalves et al., 2025; Wallnoefer et al., 2025). However, whether and how mitochondrial evolution shapes other nuclear pathways remain limited. In particular, the extent to which nuclear proteins outside the nucOXPHOS set exhibit evolutionary trajectories coordinated with mitochondrial genes is unclear, raising the question of whether mitonuclear coevolution extends beyond the canonical OXPHOS interface.

To date, a plethora of approaches to identify and evaluate coevolution exist (reviewed in Juan et al., 2013). Among them, evolutionary rate covariation (ERC) is considered one of the most successful methodologies (Pazos et al., 1997; Pazos et al., 2005). It assumes that coevolving proteins should show similar evolutionary rates (i.e., branch lengths) across a shared phylogeny, allowing the identification of proteins whose long-term evolutionary histories have been shaped by shared functional constraints (Steenwyk et al., 2022). In other words, the rates of amino acid change are expected to be similar between functionally related proteins (Clark et al., 2012; Cope et al., 2020; Little 2024). ERC has been shown to cluster proteins by pathway, reveal interaction partners, and predict functional modules without relying on prior annotations (Kowalczyk et al., 2021; Tao et al., 2024; Little et al., 2025; Forsythe et al., 2025; Gatts et al. 2026). Genome-wide ERC studies are already possible, as demonstrated by Steenwyk and colleagues (2022), who applied ERC across yeast lineages at a genomic scale. Thanks to the even greater advances in computational pipelines (Little et al., 2025; Forsythe et al., 2025), this method is predicted to be robust to noise and capable of recovering coevolving partners even when comparing protein evolutionary rates between millions of combinations.

All these features make ERC an ideal approach to explore mitonuclear coevolution beyond candidate-based analyses and to test whether (and which) other nuclear pathways track mitochondrial footprints over evolutionary timescale.

Molecular coevolution driven by physical or functional interactions can also leave detectable signatures in gene evolutionary histories, such as correlated genetic distances or partially concordant tree topologies. Based on this idea, the “mirror-tree” approach was developed to quantify the similarity between distance matrices or phylogenetic trees (Pazos and Valencia 2001, 2008; Juan et al., 2008; Juan et al., 2013; Colavin et al., 2022). Although mirror-tree similarity does not necessarily imply coevolution and can generate false positives (Sato et al., 2005), it has proven relatively robust when applied to fast-evolving markers, such as mitochondrial genes, because large amounts of signal accumulate on long branches (Gershoni et al., 2010; Barreto and Burton 2012; Pei et al., 2013; Ochoa and Pazos 2014; Formaggioni et al., 2022). This approach therefore provides a phylogenetic tree-based perspective that is conceptually distinct and complementary to ERC, which relies on covariations in evolutionary rates across a fixed species tree.

The Squamata order offers a uniquely informative system to use and combine both approaches. Their mitochondrial and nuclear phylogenies are strongly discordant in the deep node of Iguania (Acrodonta+Pleurodonta), which is supported by nuclear (and morphological) markers, and rejected by mitochondrial ones (supporting instead Acrodonta+Serpentes; Castoe et al., 2009; Wallnoefer et al., 2025). If some nuclear proteins genuinely coevolve with mitochondrial ones, their evolutionary histories should mirror the mitochondrial signal more closely than the species-tree signal. Thus, the pronounced mitonuclear discordance in Squamata provides a model to identify nuclear proteins whose phylogenetic signals could have been consistently shaped by mitonuclear coevolution dynamics.

Here, we applied both ERC and mirror tree approaches across proteomes of squamates, performing evolutionary rate covariations over 2,938,980 protein pairs and reconstructing the network of coevolving proteins. Within it, we identified and characterized communities, highlighting those that show clues of coevolution with mitochondrial proteins. In addition, we estimated the proportion of nuclear genes supporting the mitochondrial topology and quantified the proportion of those predicted to coevolve with mtOXPHOS according to ERC results.

METHODS

Data mining and orthologues search

We ensured broad taxonomic coverage across major squamate lineages mining 34 proteomes among those available in public databases, looking for a balance between taxonomic coverage and computational cost for the downstream analyses (Table S1). Due to the scope of our topological analysis, we ensured to have several representatives for three groups: Acrodonta, Pleurodonta, and Serpentes. On the other hand, we covered taxonomic diversity by selecting species distributed across Gekkota, Laterata, Anguimorpha and Scincomorpha. Additionally, we sided our nuclear dataset with complete or near-complete mitochondrial genomes for 31 species (Table S1), ensuring to have at least one mitogenomes per family. Mitochondrial genomes were retrieved from public databases when available, from previously published datasets, or reconstructed from genomic or transcriptomic resources (Table S1; Fig. S1). Specifically, three snake mitogenomes (*A. prasina, P. textilis, E. reginae*) were identified by aligning mtOXPHOS proteins from closely related species to their respective nuclear genome assemblies using the protein-to-genome aligner Miniprot (Li 2023). In one case (*N. scutatus*), mitochondrial proteins were identified by re-assembling a publicly available transcriptome (SRR519122) and querying it with DIAMOND blastx (Buchfink et al., 2015) against both the non-redundant protein database (nr; Goldfarb et al., 2025) and the *Naja naja* mitogenome (NC_010225.1). The Tuatara (S*phenodon punctatus*) was used as outgroup in all analyses.

Orthologues were identified using OrthoFinder v3.0.1b1 (Emms & Kelly 2019), retaining only the longest transcript variant per gene.

ERC analysis and networks

Whole proteome evolutionary rate covariation (ERC) analyses were performed using ERCnet (Forsythe et al., 2025). We retained only orthologues shared by at least 20 species and more than 100 amino acids long. Alignments were refined with TAPER (Zhang et al., 2021). Following the pipeline of ERCnet, gene-trees were reconciled with the species tree and ERC analysis were performed using the root-to-tip distance method.

We extracted all the orthologs predicted to coevolve according to all the combinations between Spearman's ρ (0.4, 0.5, 0.6, 0.7, 0.8 - intensity of coevolution) and p-value (0.05, 0.01, 0.001 - corrected

with the Benjamini-Hochberg False Discovery Rate; Benjamini and Hochberg 1995) cutoffs.

For each combination between Spearman's ρ and p-value, we created a coevolutionary network using custom-made Python 3.12.5 scripts. For each network, the Louvain algorithm assigned each protein to a community. Network statistics (degree, betweenness, closeness and centrality; Newman 2010) were calculated using custom-made Python 3.12.5 scripts. Node centrality medians of mitochondrial nodes were compared to a null distribution from 10,000 random samples of non-mitochondrial nodes of the same size.

We performed gene enrichment analyses on each community using topGO v2.60.1 (Alexa & Rahnenfuhrer, 2025) and a custom-made R script (R Core Team 2025). Semantic spaces were explored using ReviGO (Supek et al., 2011). The background for GO enrichments was created from the InterProScan output (--goterms --PANTHER), applied on the longest sequence of 2,424 genes used in the ERCnet pipeline.

On the other hand, we identified mitochondrial first-neighbor proteins in each network (using custom scripts). Following the same approach as above, we performed gene enrichment analyses on mitochondrial first-neighbor orthogroups (without removing mtOXPHOS). GO terms semantic clustering was performed using the HDBSCAN algorithm.

Tree inferences and topological tests

As inputs of the Squamata nuclear-based species tree inference and subsequent AU test, we used the same set of orthologs that passed Orthofinder and that was used in the first step of ERCnet (2,509 orthogroups). Firstly, we added the outgroup *S. punctatus*: this species was lacking in ERCnet because outgroups are excluded from the branch lengths covariations. After adding outgroup sequences by similarity to our already inferred orthogroups, we identified the correct outgroup copy to retain using PhyloPyPruner (--min-support 100 --min-len 100 --mask longest --prune LS; Sandberg, 2019).

Then, we retained only those orthogroups with at least one representative species for each one of the key four groups for mitonuclear discordance in Squamata: Acrodonta, Pleurodonta, Serpentes and others (Gekkota, Anguimorpha, Laterata, Scincomorpha and *S. punctatus*). A total of 2,334 orthogroups survived all these filters and were aligned and trimmed with MAFFT v7.525 (--maxiterate 1000 --localpair options; Katoh & Standley 2013) and TrimAl v1.5 (-seqoverlap 50 –resoverlap 0.5 options; Capella-Gutiérrez et al., 2009). Alignment statistics were created using AMAS (Borowiec 2016).

To determine the actual species tree, we inferred a maximum likelihood tree search via IQTREE3 (Wong et al. 2025) using partition models (-m MFP+MERGE; Lanfear et al., 2016; Kalyaanamoorthy et al., 2017) on a restricted dataset of 681 single copy, complete orthogroups including all the 31 species. Due to computational intensity, we opted for ultrafast bootstrapping in IQTREE3 (-B 1000; Hoang et al., 2018). Gene (gCF) and site (sCF) concordance factors were calculated using the --gcf and --scfl option of

IQTREE3 (Mo et al., 2023). We also computed a coalescence-based tree with ASTRAL-IV (Mirarab et al., 2014) using gene trees inferenced using IQ-TREE3 (-m MFP -mset LG -B 1,000).

On the other hand, the mitochondrial-based maximum likelihood tree was inferred from the 13 mtOXPHOS genes using partition models (-m MFP+MERGE; Lanfear et al., 2016; Kalyaanamoorthy et al., 2017) and 100 true bootstrap replicates in IQTREE3.

Each of the 2,334 proteins were used as input for the AU test wrapped in IQTREE3 (-au option; Shimodaira, 2002), where we compared the topological preference towards the nuclear-based tree or the mitochondrial-based tree. The difference among the two topologies concerns the sister relationship Acrodonta+Serpentes, that typically characterize the mitonuclear phylogenetic discordance in Squamata.

Finally, we performed gene enrichment on those nuclear proteins that supported the mitochondrial topology according to the AU result using topGO v2.60.1 (Alexa & Rahnenfuhrer, 2025) and a custom-made R script. Semantic spaces were explored using ReviGO (Supek et al., 2011). In this case, the set of 2,334 orthologs acted as background for gene enrichment.

RESULTS

Global Coevolutionary Networks and Communities Enrichment

Evolutionary rate covariation on single-copy orthologs yielded a total of 2,938,980 protein-to-protein branch length covariations, which were filtered using different combinations of p-value. All networks resulting from the combinations between Spearman's ρ and p-value are provided as Supplementary Data. For simplicity, unless otherwise specified, we will refer in the text to the network obtained under Spearman's s ρ > 0.4 and p-value < 0.05 (Fig. 1). We found that those mitochondrial genes that survived the length thresholds required to be analyzed by ERCnet (n. = 10) occupy key positions in the network. Their centrality measures are significantly greater relative to the proteome-wide background, and they can be labeled as hubs (Table S2). In fact, mitochondrial genes showed higher centrality degree (p-value = 1.4×10^{-3}), betweenness (p-value = 1.0×10^{-4}), closeness (p-value = 9.0×10^{-4}), and eigenvector centrality (p-value = 1.9×10^{-3}) (Table S2).

The Louvain algorithm identified six communities (C1–C6; Fig. 1). Community 1 (n = 526) was enriched for immune-related and extracellular signaling pathways; community 2 (n = 530) grouped proteins predominantly involved in gene regulation and neurodevelopment, with strong representation of transcriptional control processes; community 3 (n = 339) displayed significant enrichment for developmental processes and mitochondrial energy production. COX1, 2, 3, NADH1, 4, and 5 belong to Community 3.

Community 4 (n = 431) was characterized by intracellular signaling pathways, and transmembrane transport of organic acids. CYTB and ATP6 belong to this community. Community 5 (n = 113) showed a strong signal for regulation of transcription by RNA polymerase II and cardiac muscle process; finally, community 6 (n = 456) was enriched for broad metabolic processes, including organophosphate, nucleotide, carbohydrate, and amino acid metabolisms. NADH2 and NADH6 belong to this community. Complete functional enrichment results of these six communities are provided as Supplementary Data.

Mitochondrial Coevolutionary Sub-Networks

The orthogroups of NADH3, NADH4L, and ATP8 were excluded from the ERC analyses due to their short sequence length (as done for all alignments < 100 amino acids). NADH6 has by far the highest number of coevolving nuclear genes in the respective network (n = 287), while NADH4 appears to be the most isolated mitochondrial gene (n = 48) (Table S3).

For the sake of comparison, in Fig. 2 we represented two networks highlighting the first neighbors of mtOXPHOS: the first was built under relaxed thresholds (Spearman's $\rho > 0.4$ and $p < 0.05$), the second with edges passing a more severe cutoff (Spearman's $\rho > 0.7$ and $p < 0.05$). Networks resulting from the other threshold combinations are in Supplementary Data. Independently of the filter applied, mtOXPHOS first neighbors were consistently enriched for terms related to mitochondrial gene expression and transcription, and pigmentation-related processes were present in both lists (Fig. 2; Supplementary Data). Under the more relaxed filter (Spearman's $\rho > 0.4$), first neighbors showed enrichment for a broader range of metabolic and regulatory processes, including carbohydrate and glucose metabolism, glycogen and energy reserve metabolic processes, acetyl-CoA biosynthesis, autophagy of peroxisomes. In contrast, applying the more stringent filter (Spearman's $\rho > 0.7$) showed enrichment for a more specific and compact set of functions, such as lipid and fatty acid transport, calcium ion transport, terpenoid/isoprenoid metabolic processes, and intraciliary transport (Fig. 2; Supplementary Data).

Mitonuclear Phylogenetic Discordance

The nuclear-based species tree inferred from 681 loci (401,430 sites) was fully supported in all nodes and recovered the Iguania hypothesis (Fig. 3, S2; Suppl. Mat. S4). The coalescent tree confirmed this result, on the base of 2,334 nuclear orthogroups (Suppl. Mat. S4). On the contrary, the mitochondrial-based species tree inferred from 13 loci (3,426 sites) strongly supported the sister relationship Agamidae+Serpentes (Fig. 3; Suppl. Mat. S4).

The Approximately Unbiased (AU) test was applied to 2,334 nuclear orthogroups to assess support for alternative nuclear and mitochondrial topologies. Seven orthologs showed identical likelihood scores for the two topologies ($\Delta L = 0$) and were therefore considered non-informative. Among the remaining 2,327 orthologs, 1,407 (60.4%) did not significantly support either topology, whereas 809 (34.8%) and 111 (4.8%) significantly supported the nuclear and the mitochondrial topology, respectively (Fig. 3).

The ΔL measure for 11 out of 13 mtOXPHOS supports the mitochondrial topology (ΔL < 0). Such support is significant for six of them (NADH1, 2, 4, 5, COX1 and ATP6; Fig. 3). On the other hand, the ΔL measure for NADH4L and NADH6 supports the nuclear topology, but not significantly.

Gene enrichment of 111 nuclear proteins supporting the mitochondrial topology showed significant enrichment for primary metabolic processes and regulation of gene expression. In addition, among the terms directly related to mitochondrial processes are regulation of mitochondrion organization, mitochondrial ADP transmembrane transport, and regulation of action potential. Most terms referred to functions not directly related to mitochondrion. The most significative were purine nucleotide biosynthetic process, regulation of gene expression, and regionalization.

Out of these 111 nuclear proteins, only 13 participate in the stricter mitochondrial coevolutionary network as mitochondrial first-neighbors.

Proteins supporting mitochondrial topology were significantly shorter than those supporting the nuclear topology (Wilcoxon test, p-value = 1.1×10^{-14}; Fig. 3) and are composed of a lower proportion of parsimony-informative sites (Wilcoxon test, p-value = 2.2×10^{-16}; Fig. 3), while showing a lower number of gaps in the alignments (Wilcoxon test, p-value = 2.4×10^{-2}; Fig. 3).

DISCUSSION

Evolutionary rate covariation analyses have the potential to capture the signals of shared evolutionary constraints between proteins across different species (Clark et al., 2012; Priedigkeit et al., 2015). These analyses are conceptually distinct from genetic interaction networks (Costanzo et al., 2016) or gene co-expression patterns (Wisecaver et al., 2017), which primarily describe the functional associations within species in condition-dependent experiments and do not explicitly leverage the evolutionary signatures that such interactions may leave on protein sequences.

A particularly intuitive illustration of coevolution comes from reciprocal mutations that maintain structural compatibility between interacting partners (Goh et al., 2000; Kuo et al., 2010; Hill 2020; Chaurasia and Dutheil 2022; Moran et al., 2024). However, coevolution can arise also in the absence of direct binding, for instance caused by shared selective pressures, co-expression, or functional dependencies (Juan et al., 2008; Wisecaver et al., 2017; Little et al. 2024).

We generated a coevolutionary network by calculating the evolutionary rate covariation across squamates, a clade that represents an ideal model for large-scale evolutionary analyses due to its extreme phenotypic, genomic, and ecological diversity (Burbrink et al., 2020). We defined coevolving protein pairs as those showing significantly covariating evolutionary rates across the Squamata phylogeny, and tested different thresholds of Spearman's ρ (coevolution intensity) and p-value. Although evolutionary rates can be influenced by heterogeneous lineage-specific factors (Smith & Eyre-Walker 2003; Eyre-Walker & Keightley 2007), ERC nonetheless recovered a coherent and functionally interpretable coevolutionary network, where functionally related genes appeared clustered into

functional communities. Considering that Squamata span ~ 200 million years of divergence and underwent multiple episodes of lineage radiation (Zheng & Wiens 2016), the persistence of clear functional signal among communities is striking and underscores the magnitude of protein coevolution as a driver of long-term molecular evolutionary trajectories (Lovell & Robertson 2010; Carmona et al., 2015; Steenwyk et al., 2022; Gatts et al. 2026).

Given the extremely large volume of information, we prefer to focus on some functions predicted to coevolve in literature and confirm them under the light of our results.

For instance, in Community 1, functions like sperm-egg recognition, ovulation cycle, and female gonad development form a tightly connected subnetwork (Fig. 1). This reinforces the long-standing hypothesis of deep coevolution among fertilization genes, as previously demonstrated by Clark et al. (2009) in abalone, and by Findlay et al. (2014), across the *Drosophila* phylogeny. In the same community, activation of the immune response emerges alongside cellular receptors, signaling cascades, and response to stimulus, supporting a functional entanglement between innate immunity, response to stress and signal transduction (Schrom et al., 2018; Miles et al., 2019).

Another example concerns Community 2 (Fig. 1), where transcriptional regulators (such as RNA Polymerase I/II and ncRNA-mediated gene silencing), neuron differentiation and sensory organ development belong to the same community. This combination supports the linkage between regulatory complexity, gene expression control and development (Zolotarov et al., 2022; Coyle & King 2025).

Going deeper into mitonuclear coevolution, mtOXPHOS genes displayed a high number of interactions in the ERC network and spanned three communities (3, 4 and 6). Moreover, in line with previous observations (Costanzo et al., 2010; Fares et al., 2011; Costanzo et al., 2016; Steenwyk et al., 2022), our findings support that genes that participate in fundamental pathways, in this case mitochondrial OXPHOS genes, possess higher metrics (centrality degree, betweenness, closeness and eigenvector centrality; Newman 2010) compared to the background.

Among mtOXPHOS first-neighbors, the gene enrichment associated with mitochondrial transcription, peroxisomal functions, and broader energetic pathways strongly suggests the presence of an integrated coevolutionary module linking (Zhao et al., 2007; Morrison and Badyaev 2017; Koch et al., 2021). The recurrent enrichment of calcium ion import further supports this interpretation, as Ca^{2+} is a key regulator of mitochondrial activity (Cartes-Saavedra et al., 2025). Similarly, the strict relationship between mitochondria and peroxisomes is not surprising, being the mitochondrial electron transport chain a primary source of free radicals (ROS) (Demarquoy and Le Borgne 2015), and the direct role exercised by peroxisomes in response to mitochondrial oxidative stress to maintain redox homeostasis (DiGiovanni et al. 2025).

The most unexpected result is the strong enrichment for pigmentation-related proteins, which persisted even at high stringency of Spearman's ρ (> 0.8). This association may reflect an evolutionary link between mitochondrial performance, oxidative stress, and pigment synthesis. In Squamata, coloration

plays an important role in fitness-related traits, particularly in lizard courtship (Rossi et al., 2019; Batabyal et al., 2023). Pigmentation patterns are functionally differentiated, with greater color variability typically observed on the ventral surface, while dorsal hyperpigmentation contributes to protection against UV-induced damage (Griffing et al., 2020; Batabyal et al., 2023; Goldenberg et al., 2025). As in birds, ornamental coloration has been proposed to act as a signal of cellular respiratory efficiency (Johnson and Hill 2013; Weaver et al., 2018; Hill 2019). A potential mechanistic link between pigmentation and mitochondrial metabolism is provided by retinoid-dependent signaling. Beyond its established role in vision (Chen et al., 2005), retinol acts as a co-factor in the PKCδ/retinol signaling complex, which directly modulates cellular energy homeostasis by facilitating electron transfer to *cytochrome c* and regulating the efficiency of the electron transport system (Kim and Hammerling 2020). This system dynamically integrates mitochondrial redox state and metabolic demand, influencing flux through the pyruvate dehydrogenase complex and downstream Krebs cycle activity. In this light, a coordinated evolutionary response between mitochondrial OXPHOS function and pigmentation-related pathways is plausible, although this hypothesis remains speculative and should be treated with caution.

In the second part of our study, we focused on the deep mitonuclear discordance characterizing this phylum. The nuclear-based species tree inferred was fully supported in all nodes and supported the traditional Iguania hypothesis, which is widely accepted based on both morphological and molecular evidence (Burbrink et al. 2020). On the other hand, this is the third independent dataset that encountered the sister relationship between Agamidae and Serpentes using mitochondrial genes (Castoe et al., 2009; Wallnoefer et al., 2025). This discordance has been previously linked to ancient convergent evolution in oxidative phosphorylation pathways (Castoe et al., 2009; Wallnoefer et al., 2025). Because rapid mitochondrial evolution imposes compensatory pressures on physically interacting nuclear subunits, leading to accelerated evolutionary rates, some coevolving proteins might be expected to support the mitochondrial topology rather than the nuclear one. However, clear functional enrichment in mitochondrial pathways and functions, as expected, was not observed. Enrichment for terms related to chromatin organization, regionalization, and gene expression were overrepresented. In principle, a link between these functions and mitochondrial activity could be hypothesized, given the extensive influence of mitochondria across various cellular pathways. However, this interpretation remains less convincing for at least two reasons. Firstly, we would expect these functions to also emerge from the ERC analysis. Secondly, the credibility of this result is significantly weakened by the phylogenetic properties of these 111 genes (significantly shorter and with less parsimony-informative sites compared to those supporting Iguania), making them prone to stochastic discordance (Larson et al. 2026).

We hypothesize that while ERC can detect subtle rate covariation weighted by Spearman's ρ and its associated significance, the signal arising from topological test would require more pervasive and stronger coevolution to be manifested, as occurred between mitochondrial and nuclear OXPHOS (Wallnoefer et al. 2025). Such a scenario is unlikely to occur outside of direct structural or strong functional contact. Although successful applications of mirror tree theory exist (Gershoni et al., 2010; Barreto and Burton 2012; Pei et al., 2013; Ochoa and Pazos 2014), our findings suggest that topological mirroring among non-interacting proteins is rare and constrained to highly specific evolutionary contexts.

Conclusion

In this work, we characterize coevolution in Squamata through a proteome-wide ERC approach, from a general proteomic perspective to the specific case of mitochondrial OXPHOS genes. We identified functionally coherent clusters of coevolving genes and showed that mtOXPHOS genes are integrated into cellular pathways different from the evident energy production ones. Given the ancient and obligatory nature of mitonuclear interdependence in eukaryotes (Hill 2019), the strong association between mtOXPHOS and genes involved in core metabolic pathways was expected. This functional cooperation likely represents a conserved background of coevolving genes, reflecting fundamental bioenergetic and metabolic dependencies. Thus, we could hypothesize that applying a similar pipeline to other eukaryotic datasets would recover a comparable core pattern of mitonuclear associated functions, thanks to the scalability of ERC approaches to extended species and gene datasets (Little et al., 2025; Forsythe et al., 2025). At the same time, the specific signal observed between mtOXPHOS and pigmentation genes may represent a lineage-specific signature and provide evidence for the mitonuclear ecology hypothesis, suggesting that pigmentation is evolutionarily linked to mitochondrial efficiency. Although we did not directly test it, our results provide new genomic evidence to support its further exploration.

Declarations

Data Availability and Supplementary Data

All genomic data used for the present study are publicly available (Table S1). Scripts used in this study are available in the GitHub repository of the project (https://github.com/oscarwallnoefer/Squamata_Mitonuclear_Coevolution), while additional networks and gene enrichments are uploaded in the FigShare repository (https://doi.org/10.6084/m9.figshare.31455355).

Funding

This study was supported by the Italian Ministry of University and Research PRIN 2020 (2020BE2BC3) funded to M.P.

CRediT Authorship Contribution Statement

Conceptualization: OW, FP; Methodology: OW, MM, FP; Software: OW, MM, GG; Formal analysis: OW, MM; Investigation: OW, GG, NG; Data Curation: OW, GG, NG; Visualization: OW; Supervision: FP; Resources: MP; Funding acquisition: MP; Writing – Original Draft: OW, MM; Writing – Review and Editing: OW, MM, FP

Competing Interest

The authors declare that they have no known competing interests.

References

1. Alexa A, Rahnenfuhrer J (2025). topGO: Enrichment Analysis for Gene Ontology. doi:10.18129/B9.bioc.topGO, R package version 2.60.1, https://bioconductor.org/packages/topGO.
2. Barreto, F.S. and Burton, R.S., 2012. Evidence for compensatory evolution of ribosomal proteins in response to rapid divergence of mitochondrial rRNA. *Molecular biology and evolution*, *30*(2), pp.310-314.
3. Batabyal, A., Zambre, A., Mclaren, T., Rankin, K.J., Somaweera, R., Stuart-Fox, D. and Thaker, M., 2023. The extent of rapid colour change in male agamid lizards is unrelated to overall sexual dichromatism. *Ecology and Evolution*, *13*(7), p.e10293.
4. Benjamini, Y. and Hochberg, Y., 1995. Controlling the false discovery rate: a practical and powerful approach to multiple testing. *Journal of the Royal statistical society: series B (Methodological)*, *57*(1), pp.289-300.
5. Borowiec, M.L. 2016. AMAS: a fast tool for alignment manipulation and computing of summary statistics. PeerJ 4:e1660.
6. Buchfink, B., Xie, C. and Huson, D.H., 2015. Fast and sensitive protein alignment using DIAMOND. *Nature methods*, *12*(1), pp.59-60.
7. Burbrink, F.T., Grazziotin, F.G., Pyron, R.A., Cundall, D., Donnellan, S., Irish, F., Keogh, J.S., Kraus, F., Murphy, R.W., Noonan, B. and Raxworthy, C.J., 2020. Interrogating genomic-scale data for Squamata (lizards, snakes, and amphisbaenians) shows no support for key traditional morphological relationships. *Systematic biology*, *69*(3), pp.502-520.
8. Capella-Gutiérrez, S., Silla-Martínez, J. M., & Gabaldón, T. (2009). trimAl: a tool for automated alignment trimming in large-scale phylogenetic analyses. Bioinformatics (Oxford, England), 25(15), 1972–1973. https://doi.org/10.1093/bioinformatics/btp348
9. Carmona, D., Fitzpatrick, C.R. and Johnson, M.T., 2015. Fifty years of co-evolution and beyond: integrating co-evolution from molecules to species.
10. Cartes-Saavedra, B., Ghosh, A. and Hajnóczky, G., 2025. The roles of mitochondria in global and local intracellular calcium signalling. *Nature Reviews Molecular Cell Biology*, *26*(6), pp.456-475.
11. Chaurasia, S. and Dutheil, J.Y., 2022. The structural determinants of intra-protein compensatory substitutions. *Molecular Biology and Evolution*, *39*(4), p.msac063.
12. Chen, C., Tsina, E., Cornwall, M.C., Crouch, R.K., Vijayaraghavan, S. and Koutalos, Y., 2005. Reduction of all-trans retinal to all-trans retinol in the outer segments of frog and mouse rod photoreceptors. *Biophysical journal*, *88*(3), pp.2278-2287.
13. Clark, N.L., Alani, E. and Aquadro, C.F., 2012. Evolutionary rate covariation reveals shared functionality and coexpression of genes. *Genome research*, *22*(4), pp.714-720.
14. Clark, N.L., Alani, E. and Aquadro, C.F., 2013. Evolutionary rate covariation in meiotic proteins results from fluctuating evolutionary pressure in yeasts and mammals. *Genetics*, *193*(2), pp.529-538.

15. Clark, N.L., Gasper, J., Sekino, M., Springer, S.A., Aquadro, C.F. and Swanson, W.J., 2009. Coevolution of interacting fertilization proteins. *PLoS genetics*, *5*(7), p.e1000570.
16. Colavin, A., Atolia, E., Bitbol, A.F. and Huang, K.C., 2022. Extracting phylogenetic dimensions of coevolution reveals hidden functional signals. *Scientific Reports*, *12*(1), p.820.
17. Costanzo, M., Baryshnikova, A., Bellay, J., Kim, Y., Spear, E.D., Sevier, C.S., Ding, H., Koh, J.L., Toufighi, K., Mostafavi, S. and Prinz, J., 2010. The genetic landscape of a cell. *science*, *327*(5964), pp.425-431.
18. Costanzo, M., Hou, J., Messier, V., Nelson, J., Rahman, M., VanderSluis, B., Wang, W., Pons, C., Ross, C., Ušaj, M. and San Luis, B.J., 2021. Environmental robustness of the global yeast genetic interaction network. *Science*, *372*(6542), p.eabf8424.
19. Costanzo, M., VanderSluis, B., Koch, E.N., Baryshnikova, A., Pons, C., Tan, G., Wang, W., Usaj, M., Hanchard, J., Lee, S.D. and Pelechano, V., 2016. A global genetic interaction network maps a wiring diagram of cellular function. *Science*, *353*(6306), p.aaf1420.
20. Coyle, M.C. and King, N., 2025. The evolutionary foundations of transcriptional regulation in animals. *Nature Reviews Genetics*, pp.1-16.
21. Demarquoy, J. and Le Borgne, F., 2015. Crosstalk between mitochondria and peroxisomes. *World journal of biological chemistry*, *6*(4), p.301.
22. DiGiovanni, L.F., Khroud, P.K., Carmichael, R.E., Schrader, T.A., Gill, S.K., Germain, K., Jomphe, R.Y., Wiesinger, C., Boutry, M., Kamoshita, M. and Snider, D., 2025. ROS transfer at peroxisome-mitochondria contact regulates mitochondrial redox. *Science*, *389*(6756), pp.157-162.
23. Emms, D.M., Kelly, S. OrthoFinder: phylogenetic orthology inference for comparative genomics. Genome Biol 20, 238 (2019). https://doi.org/10.1186/s13059-019-1832-y
24. Fares, M.A., Ruiz-González, M.X. and Labrador, J.P., 2011. Protein coadaptation and the design of novel approaches to identify protein–protein interactions. *IUBMB life*, *63*(4), pp.264-271.
25. Findlay, G.D., Sitnik, J.L., Wang, W., Aquadro, C.F., Clark, N.L. and Wolfner, M.F., 2014. Evolutionary rate covariation identifies new members of a protein network required for Drosophila melanogaster female post-mating responses. *PLoS genetics*, *10*(1), p.e1004108.
26. Formaggioni, A., Plazzi, F. and Passamonti, M., 2022. Mito-nuclear coevolution and phylogenetic artifacts: the case of bivalve mollusks. *Scientific reports*, *12*(1), p.11040.
27. Forsythe ES, Gatts TC, Lane LE, deRoux C, Berggren MJ, Rehmann EA, Zak EN, Bartel T, L'Argent LA, Sloan DB. ERCnet: Phylogenomic Prediction of Interaction Networks in the Presence of Gene Duplication. Mol Biol Evol. 2025 Apr 30;42(5):msaf089. doi: 10.1093/molbev/msaf089. PMID: 40247660; PMCID: PMC12062884.
28. Gatts, T.C., Rehmann, E.A., Lane, L.E., Sloan, D.B. and Forsythe, E.S., 2026. Correlated evolutionary rates reveal novel components and cross-compartment connectivity in plant proteostasis systems. *Genome Biology and Evolution*, *18*(2), p.evag007.
29. Gershoni, M., Fuchs, A., Shani, N., Fridman, Y., Corral-Debrinski, M., Aharoni, A., Frishman, D. and Mishmar, D., 2010. Coevolution predicts direct interactions between mtDNA-encoded and nDNA-

encoded subunits of oxidative phosphorylation complex I. *Journal of molecular biology*, *404*(1), pp.158-171.

30. Goh, C.S., Bogan, A.A., Joachimiak, M., Walther, D. and Cohen, F.E., 2000. Co-evolution of proteins with their interaction partners. *Journal of molecular biology*, *299*(2), pp.283-293.
31. Goldenberg, J., Bisschop, K., Lambert, J.W., Nicolaï, M.P., Etienne, R.S., D'Alba, L. and Shawkey, M.D., 2025. Habitat openness and squamate color evolution over deep time. *Nature Communications*, *16*(1), p.2625.
32. Goldfarb T, Kodali VK, Pujar S, Brover V, Robbertse B, Farrell CM, Oh DH, Astashyn A, Ermolaeva O, Haddad D, Hlavina W, Hoffman J, Jackson JD, Joardar VS, Kristensen D, Masterson P, McGarvey KM, McVeigh R, Mozes E, Murphy MR, Schafer SS, Souvorov A, Spurrier B, Strope PK, Sun H, Vatsan AR, Wallin C, Webb D, Brister JR, Hatcher E, Kimchi A, Klimke W, Marchler-Bauer A, Pruitt KD, Thibaud-Nissen F, Murphy TD. NCBI RefSeq: reference sequence standards through 25 years of curation and annotation. Nucleic Acids Res. 2025 Jan 6;53(D1):D243-D257
33. Gonçalves, L.T., Pezzi, P.H., Deprá, M. and Françoso, E., 2025. Mitonuclear coevolution in bumblebees (Bombus): genomic signatures and its role in climatic niche adaptation. *Genome Biology and Evolution*, *17*(7), p.evaf123.
34. Griffing, A.H., Gamble, T. and Bauer, A.M., 2020. Distinct patterns of pigment development underlie convergent hyperpigmentation between nocturnal and diurnal geckos (Squamata: Gekkota). *BMC Evolutionary Biology*, *20*(1), p.40.
35. Hidetoshi Shimodaira, An Approximately Unbiased Test of Phylogenetic Tree Selection, Systematic Biology, Volume 51, Issue 3, 1 May 2002, Pages 492–508, https://doi.org/10.1080/10635150290069913
36. Hill, G.E., 2019. *Mitonuclear ecology*. Oxford University Press.
37. Hill, G.E., Hood, W.R., Ge, Z., Grinter, R., Greening, C., Johnson, J.D., Park, N.R., Taylor, H.A., Andreasen, V.A., Powers, M.J. and Justyn, N.M., 2019. Plumage redness signals mitochondrial function in the house finch. *Proceedings of the Royal Society B*, *286*(1911), p.20191354.
38. Hill, G.E., 2020. Mitonuclear compensatory coevolution. *Trends in Genetics*, *36*(6), pp.403-414.
39. Hoang, D.T., Chernomor, O., Von Haeseler, A., Minh, B.Q. and Vinh, L.S., 2018. UFBoot2: improving the ultrafast bootstrap approximation. *Molecular biology and evolution*, *35*(2), pp.518-522.
40. Johnson, J.D. and Hill, G.E., 2013. Is carotenoid ornamentation linked to the inner mitochondria membrane potential? A hypothesis for the maintenance of signal honesty. *Biochimie*, *95*(2), pp.436-444.
41. Juan, D., Pazos, F. and Valencia, A., 2008. High-confidence prediction of global interactomes based on genome-wide coevolutionary networks. *Proceedings of the National Academy of Sciences*, *105*(3), pp.934-939.
42. Juan, D., Pazos, F. and Valencia, A., 2013. Emerging methods in protein co-evolution. *Nature Reviews Genetics*, *14*(4), pp.249-261.

43. Kalyaanamoorthy, S., Minh, B.Q., Wong, T.K., Von Haeseler, A. and Jermiin, L.S., 2017. ModelFinder: fast model selection for accurate phylogenetic estimates. *Nature methods*, *14*(6), pp.587-589.
44. Katoh K, Standley DM. MAFFT multiple sequence alignment software version 7: improvements in performance and usability. Mol Biol Evol. 2013 Apr;30(4):772-80. doi: 10.1093/molbev/mst010.
45. Kim, Y.K. and Hammerling, U., 2020. The mitochondrial PKCδ/retinol signal complex exerts real-time control on energy homeostasis. *Biochimica et Biophysica Acta (BBA)-Molecular and Cell Biology of Lipids*, *1865*(11), p.158614.
46. Koch, R.E., Buchanan, K.L., Casagrande, S., Crino, O., Dowling, D.K., Hill, G.E., Hood, W.R., McKenzie, M., Mariette, M.M., Noble, D.W. and Pavlova, A., 2021. Integrating mitochondrial aerobic metabolism into ecology and evolution. *Trends in Ecology & Evolution*, *36*(4), pp.321-332.
47. Kowalczyk, A., Gbadamosi, O., Kolor, K., Sosa, J., Andrzejczuk, L., Gibson, G., St Croix, C., Chikina, M., Aizenman, E., Clark, N. and Kiselyov, K., 2021. Evolutionary rate covariation identifies SLC30A9 (ZnT9) as a mitochondrial zinc transporter. *Biochemical Journal*, *478*(17), pp.3205-3220.
48. Kuo, D., Licon, K., Bandyopadhyay, S., Chuang, R., Luo, C., Catalana, J., Ravasi, T., Tan, K. and Ideker, T., 2010. Coevolution within a transcriptional network by compensatory trans and cis mutations. *Genome research*, *20*(12), pp.1672-1678.
49. Larson, D.A., Itgen, M.W., Denton, R.D. and Hahn, M.W., 2026. Reconsidering cytonuclear discordance in the genomic age. *Evolution*, *80*(1), pp.1-14.
50. Li, H., 2023. Protein-to-genome alignment with miniprot. Bioinformatics, 39, btad014
51. Little, J., Chikina, M. and Clark, N.L., 2024. Evolutionary rate covariation is a reliable predictor of co-functional interactions but not necessarily physical interactions. *Elife*, *12*, p.RP93333.
52. Little, J., Meyer, G.H., Grover, A., Francette, A.M., Partha, R., Arndt, K.M., Smith, M., Clark, N. and Chikina, M., 2025. ERC 2.0-evolutionary rate covariation update improves inference of functional interactions across large phylogenies. *bioRxiv*.
53. Lovell, S.C. and Robertson, D.L., 2010. An integrated view of molecular coevolution in protein–protein interactions. *Molecular biology and evolution*, *27*(11), pp.2567-2575.
54. Miles, J., Scherz-Shouval, R. and van Oosten-Hawle, P., 2019. Expanding the organismal proteostasis network: linking systemic stress signaling with the innate immune response. *Trends in biochemical sciences*, *44*(11), pp.927-942.
55. Minh, B.Q., Schmidt, H.A., Chernomor, O., Schrempf, D., Woodhams, M.D., Von Haeseler, A. and Lanfear, R., 2020. IQ-TREE 2: new models and efficient methods for phylogenetic inference in the genomic era. *Molecular biology and evolution*, *37*(5), pp.1530-1534.
56. Mo, Y.K., Lanfear, R., Hahn, M.W. and Minh, B.Q., 2023. Updated site concordance factors minimize effects of homoplasy and taxon sampling. *Bioinformatics*, *39*(1), p.btac741.
57. Moran, B.M., Payne, C.Y., Powell, D.L., Iverson, E.N., Donny, A.E., Banerjee, S.M., Langdon, Q.K., Gunn, T.R., Rodriguez-Soto, R.A., Madero, A. and Baczenas, J.J., 2024. A lethal mitonuclear incompatibility in complex I of natural hybrids. *Nature*, *626*(7997), pp.119-127.

58. Morrison, E.S. and Badyaev, A.V., 2017. Beyond topology: coevolution of structure and flux in metabolic networks. *Journal of Evolutionary Biology*, *30*(10), pp.1796-1809.
59. Newman, M.E., 2010. Networks: an introduction.
60. Ochoa, D. and Pazos, F., 2014. Practical aspects of protein co-evolution. *Frontiers in cell and developmental biology*, *2*, p.14.
61. Pazos, F. and Valencia, A., 2001. Similarity of phylogenetic trees as indicator of protein–protein interaction. *Protein engineering*, *14*(9), pp.609-614.
62. Pazos, F. and Valencia, A., 2008. Protein co-evolution, co-adaptation and interactions. *The EMBO journal*, *27*(20), pp.2648-2655.
63. Pazos, F., Helmer-Citterich, M., Ausiello, G. and Valencia, A., 1997. Correlated mutations contain information about protein-protein interaction. *Journal of molecular biology*, *271*(4), pp.511-523.
64. Pazos, F., Ranea, J.A., Juan, D. and Sternberg, M.J., 2005. Assessing protein co-evolution in the context of the tree of life assists in the prediction of the interactome. *Journal of molecular biology*, *352*(4), pp.1002-1015.
65. Pei, Z.Y., Mu, G.L., Pan, J. and Zhang, D.M., 2013. Codon usage and coevolution of the large and small subunits of ribulose-1, 5-bisphosphate carboxylase/oxygenase. *Journal of Systematics and Evolution*, *51*(5), pp.511-521.
66. Priedigkeit, N., Wolfe, N. and Clark, N.L., 2015. Evolutionary signatures amongst disease genes permit novel methods for gene prioritization and construction of informative gene-based networks. *PLoS genetics*, *11*(2), p.e1004967.
67. R Core Team (2025). R: A Language and Environment for Statistical Computing. R Foundation for Statistical Computing, Vienna, Austria. <https://www.R-project.org/>.
68. Rossi, N., Benitez-Vieyra, S., Cocucci, A., Chiaraviglio, M. and Cardozo, G., 2019. Sexual dichromatism and color diversity in the spiny lava lizard Tropidurus spinulosus using lizard visual modelling. *Scientific reports*, *9*(1), p.14270.
69. Sandberg, F. 2019. *PhyloPyPruner: Tree-based orthology inference with functionality for reducing contamination*: https://github.com/fethalen/phylopypruner (accessed April 2025).
70. Sato, T., Yamanishi, Y., Kanehisa, M. and Toh, H., 2005. The inference of protein–protein interactions by co-evolutionary analysis is improved by excluding the information about the phylogenetic relationships. *Bioinformatics*, *21*(17), pp.3482-3489.
71. Schrom, E.C., Prada, J.M. and Graham, A.L., 2018. Immune signaling networks: sources of robustness and constrained evolvability during coevolution. *Molecular biology and evolution*, *35*(3), pp.676-687.
72. Shimodaira, H., 2002. An approximately unbiased test of phylogenetic tree selection. *Systematic biology*, *51*(3), pp.492-508.
73. Sloan, D.B., Warren, J.M., Williams, A.M., Wu, Z., Abdel-Ghany, S.E., Chicco, A.J. and Havird, J.C., 2018. Cytonuclear integration and co-evolution. *Nature Reviews Genetics*, *19*(10), pp.635-648.

74. Steenwyk, J.L., Phillips, M.A., Yang, F., Date, S.S., Graham, T.R., Berman, J., Hittinger, C.T. and Rokas, A., 2022. An orthologous gene coevolution network provides insight into eukaryotic cellular and genomic structure and function. *Science Advances*, *8*(18), p.eabn0105.
75. Supek F, Bošnjak M, Škunca N, Šmuc T. REVIGO summarizes and visualizes long lists of gene ontology terms. PLoS One. 2011;6(7):e21800. doi: 10.1371/journal.pone.0021800. Epub 2011 Jul 18. PMID: 21789182; PMCID: PMC3138752.
76. Tao, M., Chen, J., Cui, C., Xu, Y., Xu, J., Shi, Z., Yun, J., Zhang, J., Ou, G.Z., Liu, C. and Chen, Y., 2024. Identification of a longevity gene through evolutionary rate covariation of insect mito-nuclear genomes. *Nature Aging*, *4*(8), pp.1076-1088.
77. Weaver, R.J., Santos, E.S., Tucker, A.M., Wilson, A.E. and Hill, G.E., 2018. Carotenoid metabolism strengthens the link between feather coloration and individual quality. *Nature communications*, *9*(1), p.73.
78. Williams, T.A. and Embley, T.M., 2014. Archaeal "dark matter" and the origin of eukaryotes. *Genome Biology and Evolution*, *6*(3), pp.474-481.
79. Wisecaver, J.H., Borowsky, A.T., Tzin, V., Jander, G., Kliebenstein, D.J. and Rokas, A., 2017. A global coexpression network approach for connecting genes to specialized metabolic pathways in plants. *The Plant Cell*, *29*(5), pp.944-959.
80. Wong, T.K., Ly-Trong, N., Ren, H., Baños, H., Roger, A.J., Susko, E., Bielow, C., De Maio, N., Goldman, N., Hahn, M.W. and Huttley, G., 2025. IQ-TREE 3: Phylogenomic Inference Software using Complex Evolutionary Models.
81. Yan, Z., Ye, G. and Werren, J.H., 2019. Evolutionary rate correlation between mitochondrial-encoded and mitochondria-associated nuclear-encoded proteins in insects. *Molecular Biology and Evolution*, *36*(5), pp.1022-1036.
82. Zhang, C., Zhao, Y., Braun, E. L., & Mirarab, S. (2021). TAPER: Pinpointing errors in multiple sequence alignments despite varying rates of evolution. Methods in Ecology and Evolution, 00, 1– 14. https://doi.org/10.1111/2041-210X.13696
83. Zhao, J., Ding, G.H., Tao, L., Yu, H., Yu, Z.H., Luo, J.H., Cao, Z.W. and Li, Y.X., 2007. Modular co-evolution of metabolic networks. *BMC bioinformatics*, *8*(1), p.311.
84. Zolotarov, G., Fromm, B., Legnini, I., Ayoub, S., Polese, G., Maselli, V., Chabot, P.J., Vinther, J., Styfhals, R., Seuntjens, E. and Di Cosmo, A., 2022. MicroRNAs are deeply linked to the emergence of the complex octopus brain. *Science advances*, *8*(47), p.eadd9938.

Figures

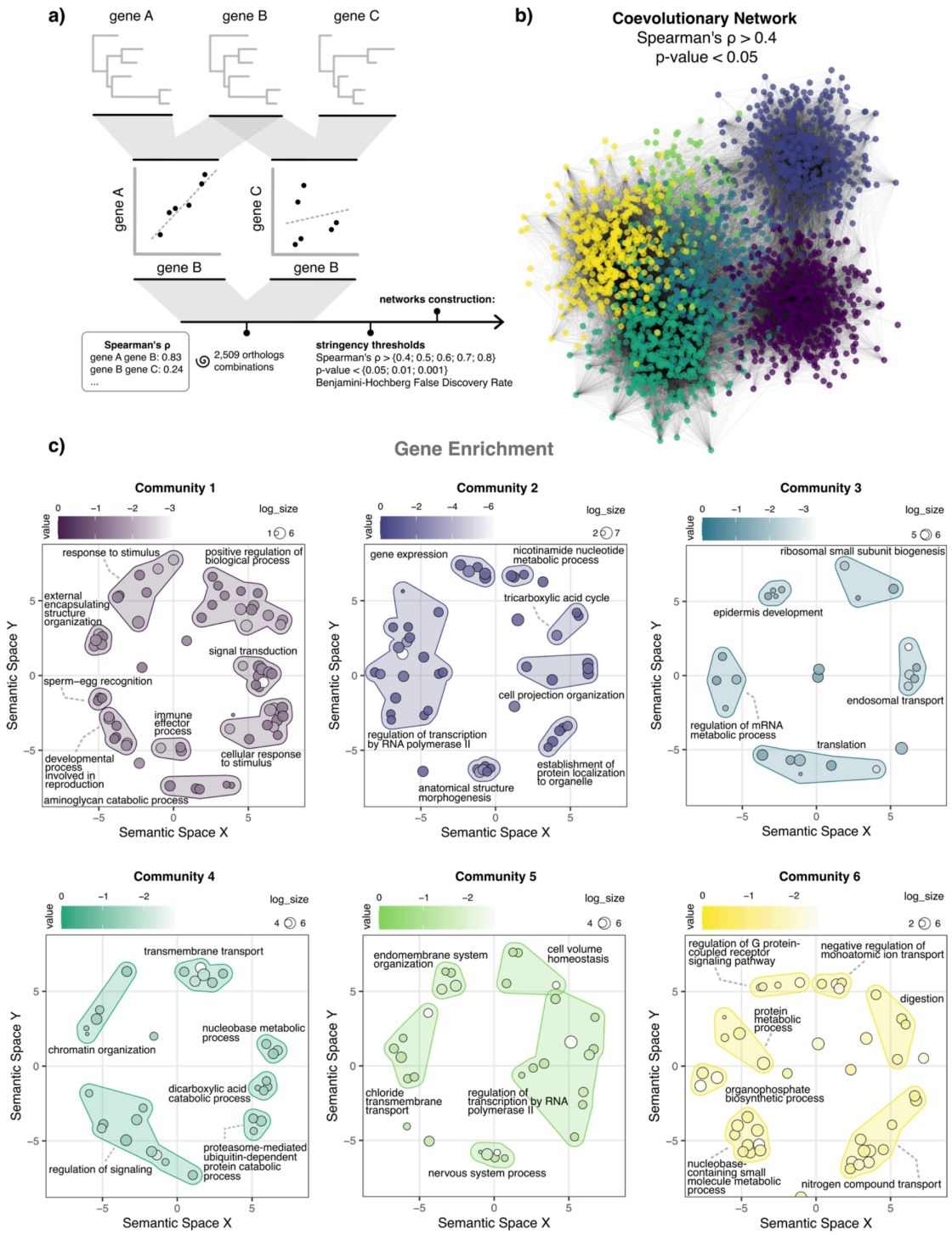


Figure 1

a) Rationale behind evolutionary rates covariation (ERC): coevolving genes show correlated branch lengths along gene-tree phylogenies. Putative coevolving genes can be represented as a network. ERC was performed using the pipeline ERCnet (Forsythe et al. 2025). **b)** Coevolutionary network passing Spearman's ρ > 0.4 and p-value < 0.05. Each color represents a community (n = 6). **c)**Graphical

representation of gene functional enrichment resulting from each community. The most frequent term is used for labeling each cluster. Colors are referred to the communities in b).

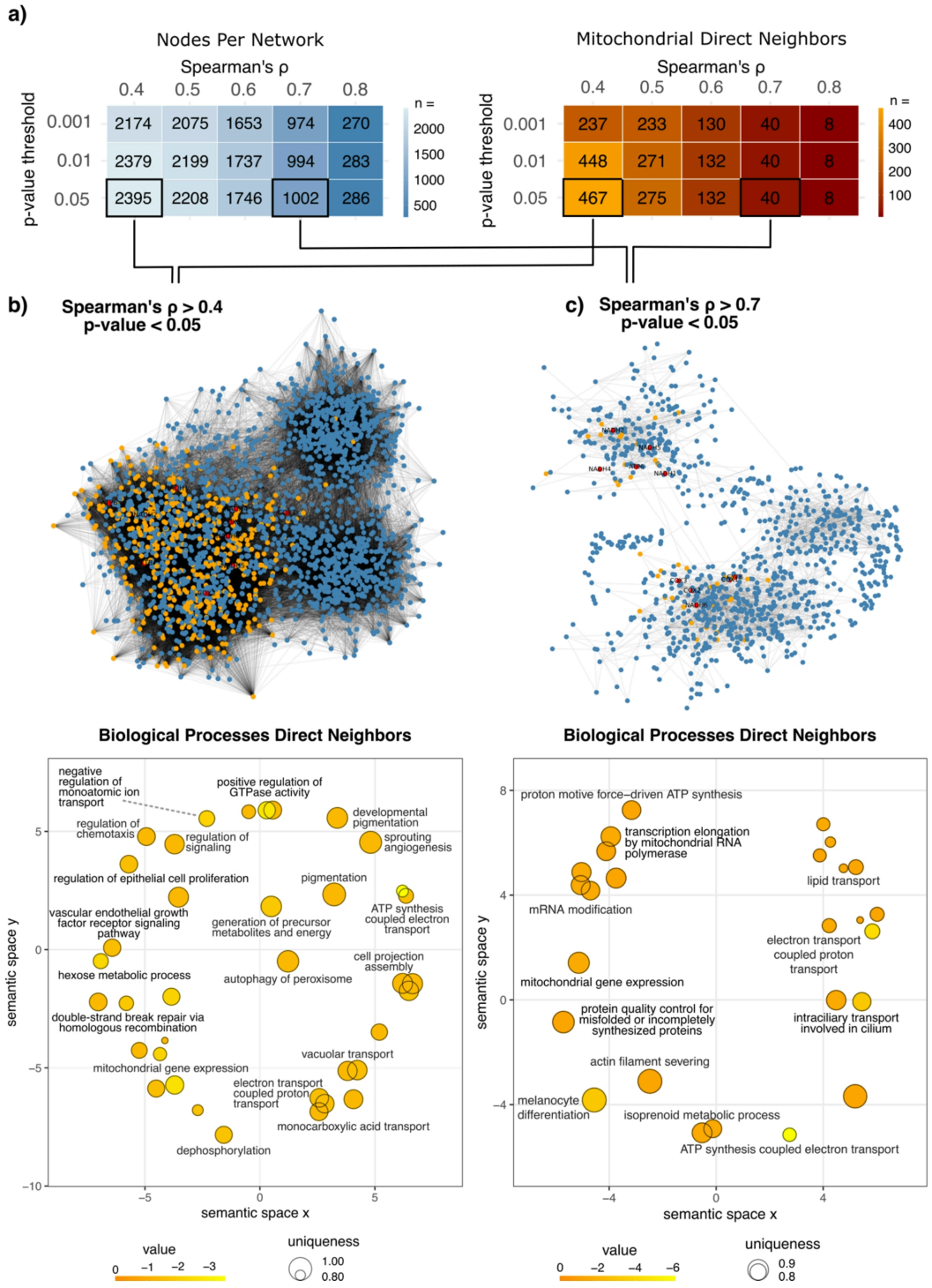


Figure 2

a) Numbers of nodes per network, according to Spearman's ρ and p-value thresholds. The table on the left shows the total number of nodes per network. The table on the right shows the number of nodes that are direct neighbors of at least one mtOXPHOS node. **b)**Network with p-value < 0.05 and Spearman's ρ >

0.4. **c)** Network with p-value < 0.05 and Spearman's ρ > 0.7. mtOXPHOS nodes are highlighted in red, and their direct neighbors in yellow. Under each network, gene functional enrichment resulting from mitochondrial direct neighbors is shown. Points with dispensability < 0.25 are labeled (dispensability measures GO term redundancy based on semantic similarity).

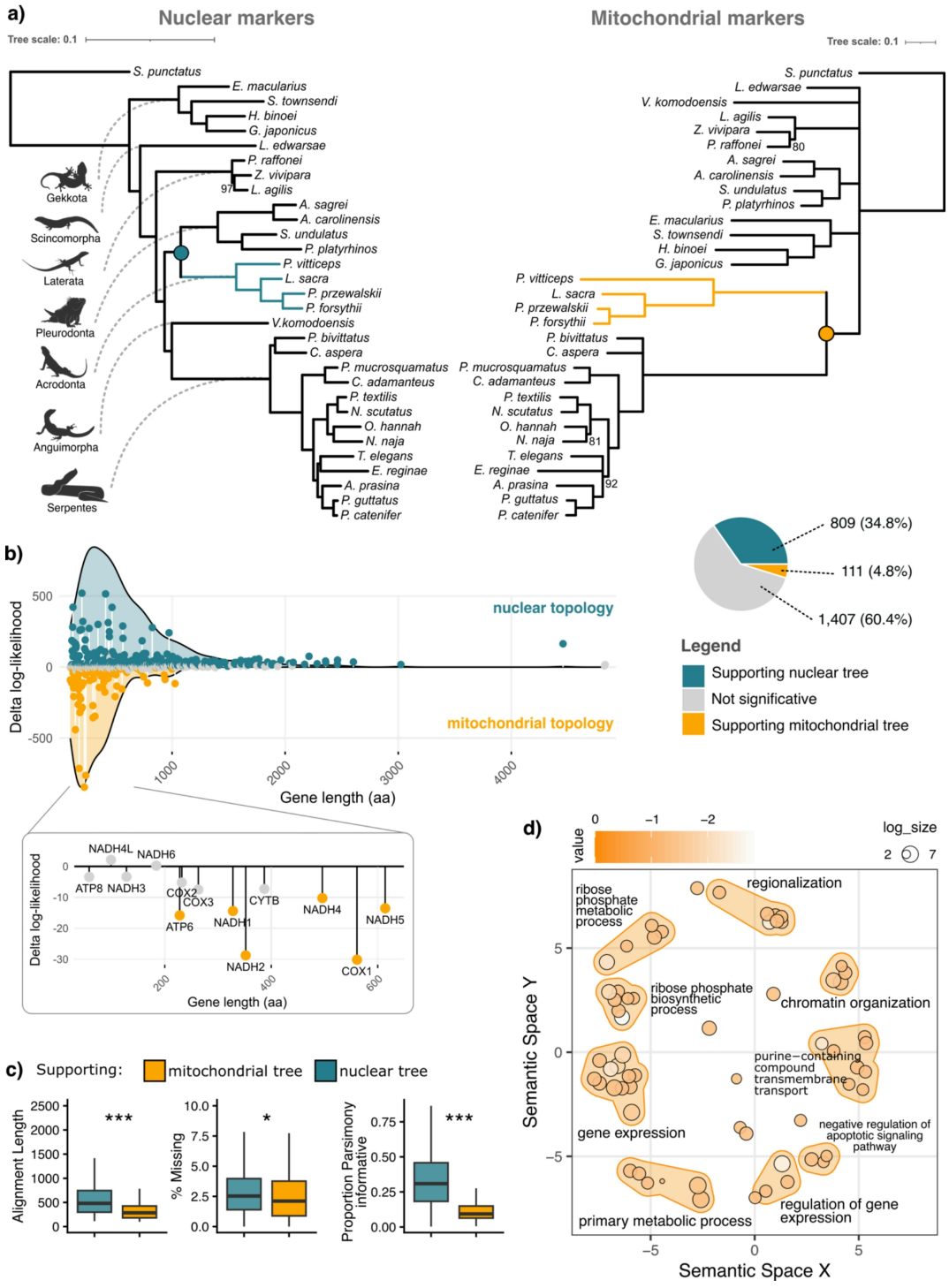


Figure 3

(a) Maximum likelihood trees of Squamata inferred from nuclear (left; 681 loci) and mitochondrial (right; 13 loci) markers. mtOXPHOS proteins support a sister-group relationship between Agamidae (Acrodonta) and Serpentes. Node supports are shown if bootstrap proportion < 100. **(b)** AU test on 2,327 gene trees between nuclear and mitochondrial topologies. Points are sorted by protein length. Genes supporting nuclear topology are shown in green (ΔL > 0), while those supporting the mitochondrial topology in orange (ΔL < 0), and non-significant genes in grey. The AU test applied to the 13 mtOXPHOS genes is shown in the window. The proportion of proteins supporting each topology is shown in the pie chart. **c)** Alignment statistics (gene length, percentage of gaps, proportion of parsimony informative sites) for the gene dataset used for the AU test. **d)** Gene enrichment analysis performed on the biological processes of the nuclear proteins (n = 111) supporting the mitochondrial topology. Semantic clustering was performed using the HDBSCAN algorithm. The most frequent term was used for labeling each cluster.

Supplementary Files

This is a list of supplementary files associated with this preprint. Click to download.

- SupplementaryMaterials.docx